공학석사 학위논문

Development of Optical Biomedical Signal Monitoring Module for Unconstrained Pulse Oxymetry and Portable fNIRS

무구속 Pulse Oxymetry와 휴대용 fNIRS 구현을 위한 광학적 생체신호 측정 시스템 개발

2012 년 8 월

서울대학교 대학원
협동과정 바이오엔지니어링 전공
이 종 민

Development of Optical Biomedical Signal Monitoring Module for Unconstrained Pulse Oxymetry and Portable fNIRS

지도 교수 박 광 석

이 논문을 공학석사 학위논문으로 제출함

2012 년 6 월

서울대학교 대학원

협동과정 바이오엔지니어링 전공

이 종 민

이종민의 공학석사 학위논문을 인준함

2012 년 6 월

위 원 장 김 희 찬 (인)

부위원장 박 광 석 (인)

위 원 김 성 완 (인)

학위논문 원문제공 서비스에 대한 동의서

본인의 학위논문에 대하여 서울대학교가 아래와 같이 학위논문 저작물을 제공하는 것에 동의합니다.

1. 동의사항

①본인의 논문을 보존이나 인터넷 등을 통한 온라인 서비스 목적으로 복제할 경우 저작물의 내용을 변경하지 않는 범위 내에서의 복제를 허용합니다.

②본인의 논문을 디지털화하여 인터넷 등 정보통신망을 통한 논문의 일부 또는 전부의 복제.배포 및 전송 시 무료로 제공하는 것에 동의합니다.

2. 개인(저작자)의 의무

본 논문의 저작권을 타인에게 양도하거나 또는 출판을 허락하는 등 동의 내용을 변경하고자 할 때는 소속대학(원)에 공개의 유보 또는 해지를 즉시 통보하겠습니다.

3. 서울대학교의 의무

①서울대학교는 본 논문을 외부에 제공할 경우 저작권 보호장치(DRM)를 사용하여야 합니다.

②서울대학교는 본 논문에 대한 공개의 유보나 해지 신청 시 즉시 처리해야 합니다.

논문제목 : 무구속 Pulse Oxymetry와 휴대용 fNIRS 구현을 위한 광학적 생체신호 측정 시스템 개발

학위구분 : **석사 ■.박사 □**
학 과 : 공과대학 협동과정 바이오엔지니어링 전공
학 번 : 2010-23354
연 락 처 : emmaneul.lee@ti.com
저 작 자 : 이 종 민 이종민

제 출 일 : 2012 년 8월 3일

서울대학교총장 귀하

Abstract

Development of Optical Biomedical Signal Monitoring Module for Unconstrained Pulse Oxymetry and Portable fNIRS

Jongmin Lee

Interdisciplinary Program in Bioengineering
Seoul National University

This thesis describes the development of optical measurement module to monitor optical biomedical signals in an unconstrained manner and its application to unconstrained pulse oximetry and portable functional near infrared spectroscopy (fNIRS).

The system's light source is power light emitting diode (power LED) based while its detector is PIN Diode based, and power LED operated in peak forward modulation. Power LED lowered the spatial error by putting the dies of the two waves (760nm and 880nm) into one package. In order for the intensity of light and measured signals to adapt to the environment, the light intensity was adjusted with adaptive light intensity control technique.

The non-intrusive pulse oximeter, which adopts this module, is made as reflection type that allows the oximeter to be equipped onto chairs or beds, and SpO2 was qualitatively measured with ratio to ratio that differs by the absorbance of each wave. The experiment was conducted in a way that

examined the two waves and measured the reflected signals under a condition of wearing clothes, thin and thick respectively. As a result, the signals from two different waves could be measured separately, thus SpO2 and cardiac impulse could be calculated through the detection of the high peak and low peak of each wave. Since the light intensity was automatically adjusted to the environment, it was confirmed that diminishment or saturation of the measured signals was prevented.

The light source and detector of Portable fNIRS using this module are separated in order to be flexibly applied to each of the frontal, motor cortex and occipital of the cerebrum.

In order to confirm the application of the system, the fNIRS was applied to Cz and finger tapping tests with different timeframe were conducted. This confirmed the clear gap between the signals of the finger tapping and resting section.

Keywords : portable, non-intrusive, optical biomedical signal monitoring, pulse oximetry, functional near-infrared spectroscopy

Student number : 2010-23354

Contents

List of Tables

List of Figures

Chapter 1. Introduction

Hemodynamics monitoring technique using IR range light has been grown certainly for past several decades. Pulse oximetry is classic example of these applications and widely used in the clinical field for oxygen saturation of arterial blood monitoring since it was introduced in 1983.[1] This technique is also widely used in various field of medicine such as optical mammography, functional brain monitoring, etc.[2]

My target was developing unconstrained pulse oximeter and portable fNIRS Module. However conventional oxygen saturation monitoring methods have several problems to make these modules in a way. In this chapter deal with the motivation, scientific background, review the conventional technologies and its required complements for the new modules.

1.1 Motivation

Non-invasive and non-intrusive biomedical signal monitoring techniques such as capacitive coupled electrocardiogram, ballistocardiogram in daily life have developed evidently for the past several years. However, oxygen saturation monitoring system for ubiquitous healthcare has not yet developed.[3] Also, even though there are several portable fNIRS machine, there is no potable fNIRS machine for motor cortex or occipital cortex yet.

For the non-intrusive pulse oximetry, the system can be embedded in daily life contacted furniture such as chair and bed. Also, the light intensity needs to be enough high for penetrating various thickness of clothes. In case of portable fNIRS, it should be like a cap form so easy to be worn and operated. In addition to this, it should not only have high light intensity and sensitive detectors but also be small enough to carry.

The key technologies for these two systems are very similar. Those are coupling of adequate light emitter & detector and its appropriate control. So, I reviewed possible light emitter and detector based on its performance and volume, also designed light intensity control and signal processing technique for making above relatively new concept module.

1.2 Background

1.2.1 Light Absorption and Scattering in Tissue

1.2.1.1 Optical Window

The Optical window (also known as therapeutic window) defines the range of wavelengths where light has its maximum depth of penetration in tissue. Within the NIR window, scattering is the most dominant light−tissue interaction, and therefore the propagating light becomes diffuse rapidly. Since scattering increases the distance travelled by photons within tissue, the probability of photon absorption also increases. Because scattering has weak dependence on wavelength, the optical window is primarily limited by absorption, due to either blood at short wavelengths or water at long wavelengths.[4] So, NIR are being used in various clinical instruments.

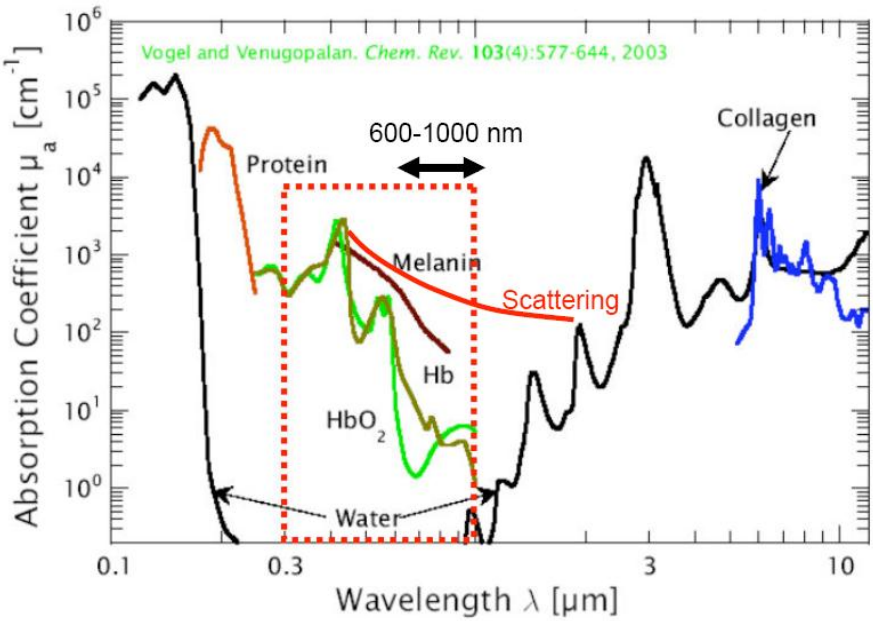

Figure 1−1. Optical window in biological tissue [4]

1.2.1.2 The Beer–Lambert Law

Layers of a substance of equal thickness each absorb the same fraction of an incident beam of light. Thus in a medium consisting of three layers, if the first absorbs ½ of the incident light, the second will absorb ½ the remaining light, as will the third layer, and only ⅛ of the incident light will emerge from the third layer. This law, derived in the 18th century, is commonly known as the Lambert–Bouguer law, and describes the logarithmic attenuation of light travelling through an absorbing medium. The Lambert–Bouguer can be written as,

$$I = I_0 e^{-cd} \qquad (1-1)$$

$$A = \ln (I_0/I) = \alpha c d \qquad (1-2)$$

The dimensionless term A is the light attenuation, given nominal units of optical density (OD), that indicates the order of magnitude of attenuation between the incident light I_0 and the transmitted light I. α and c are respectively, the absorptivity (μmolar^{-1} cm^{-1}) and concentration of the absorbing substance, and d is the distance between the points where the light enters and exits the medium.

In cases where there are multiple absorbing substances dissolved in a non–absorbing medium, the combined attenuation due to all the absorbing substance is given by the sum of their individual contributions multiplied by the length of the path travelled by the light, that is,

$$A = [\alpha_1 c_1 d + \alpha_2 c_2 d + \cdots + \alpha_n c_n d] \qquad (1-3)$$

In a typical spectroscopic application, it is required to determine the concentrations of a certain number of substances

each of which has a different absorptivity at different wavelengths. The absorptivity as a function of wavelength is known for each absorber and the distance d can be measured. Then for different wavelengths of light the attenuation of the medium is measured experimentally. Provided the number of wavelengths used is at least equal to the number of absorbing substances, the concentrations of each of the substances can be found by solving the resulting set of simultaneous equations.[5]

1.2.1.3 The Modified Beer-Lambert Law

Of the observed attenuation by tissue between two points, absorption accounts for only about 20%, with scattering accounting for the remaining 80%. The Beer-Lambert law can be modified to take account of the effects of scattering by including an additive term G-the attenuation due to scattering, and a multiplicative term B-the differential path length factor, which when multiplied by the geometric distance d between the source and detector, accounts for the increase in optical path length caused by scattering. Thus the modified Beer-Lambert law can be written as

$$A = \ln (I_0/I) = \alpha c d B + G \qquad (1-4)$$

The scattering loss G is usually unknown and is dependent on the relative positions of the source and detector, and on the scattering coefficient of the tissue under investigation. As a result of the unknown term, the modified law cannot be used in the same way as the original law, to generate simultaneous equations yielding quantitative values for the sought concentrations. Instead the equation (1-1) is used in a differential form in which the scattering loss is considered to be constant for a given source and detector position. A

measurement is made at a particular wavelength yielding attenuation A_1 corresponding to concentration level c_1. Sometime later, the concentration of the chromophore has changed to c_2; another measurement is taken yielding attenuation A_2. Provided the loss due to scattering (G), the geometric distance between source and detector (d), and the differential path length factor (B), are the same for each measurement, the change in concentration $\Delta c = (c_2 - c_1)$ can be calculated as

$$\Delta A = (A_2 - A_1) = \Delta c \alpha dB \qquad (1-5)$$

For multiple chromophores measured at wavelength λ, the differential attenuation can be written as

$$\Delta A(\lambda) = [\alpha_1(\lambda)\Delta c_1 + \cdots + \alpha_n(\lambda)\Delta c_n] dB(\lambda) \qquad (1-6)$$

where $\alpha_n(\lambda)$ is the absorption of nth chromophore present in the medium measured at a wavelength λ, and where c_n is the concentration of that chromophore in the medium.[5]

1.2.2 Pulse Oximetry

1.2.2.1 Prior Art of Pulse Oximeters

There are many models and brands of pulse oximeters. A sampling based on popularity and features was chosen. The models described cover the full gamut of possible feature sets, from completely wired and stationary units, to highly portable disaster-relief and triage models, to Bluetooth-compatible wireless units.[6]

(a) (b)

(c) (d)

Figure 1-2. Prior art of pulse oximetry (a) Nonin Avant 9700 (b) Nonin Avant 4000 (c) GE TruSat (d) Nonin Onyx 9500

Table 1-1. Pulse oximeter model comparison

Model	Batteries/Power	Battery Life	Telemetry Standard	Telemetry Range	Pleth Wave	Accuracy	Cost
Avant 4000 (Nonin)	Two AA batteries Tx, AC/Rech Bat display	>120 hours Tx, 18 hours display	Point to Point BlueTooth, 2.4GHz	10m	No	2% SPO2, 3% Pulse	$1,650
Nonin WristOx	Two 1.5V N-cell	24 hours	NA	NA	No	2% SPO2, 3% Pulse	$725
Avant 9700 (Nonin)	AC/Rech Bat	12 hours	NA	NA	Yes	2% SPO2, 3% Pulse	$1,995
SPO 75008	3.6V Lithium	300 hours	NA	NA	No	2% SPO2, 3% Pulse	$499
GE TruSat	AC/Rech Bat	20 hours	NA	NA	No	2% SPO2, 2% Pulse	$1,895
Philips Intellivue	Two AA batteries	17 hours	DECT, 1.4GHz	35m	No	2% SPO2, 3% Pulse	*Unknown, units bought as a cellular infrastructure*

1.2.2.2 Calculation of Arterial Blood Oxygen Saturation

Arterial oxygen saturation, SpO2, is the ratio of oxy-hemoglobin to total hemoglobin. That is,

$$SpO2 = \frac{[HbO]}{[HbO]+[HbR]} \times 100\% \qquad (1-7)$$

The subscript p denotes the arterial oxygen saturation as measured by a pulse oximeter. HbO and HbR is oxygenated and reduced hemoglobin respectively.
If we only consider [HbO] and [HbR] in Arterial blood, equation (1-7) can be equation (1-8).

$$\Delta A = (\alpha HbO \ \Delta[HbO] + \alpha HbR \ \Delta[HbR])\ dB \qquad (1-8)$$

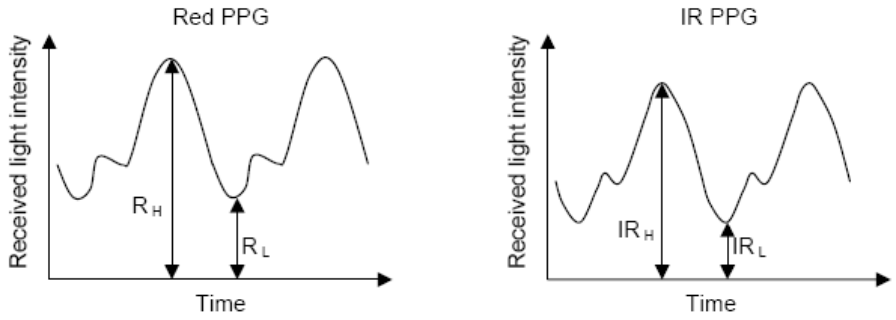

Figure 1-3. Received light intensity from the red (R) and infrared (IR) [5]

For calculating each two concentration change (⊿[HbO], ⊿[HbR]), at least two wavelength are needed. We choose 760nm, 880nm IR wavelength respectively. The reason why we choose these two wavelengths are i) these are in the optical window range ii) we use same photo detector for each wavelength so, smaller wavelength difference between two wavelengths is better. iii) Each wavelength is separated by isosbestic point of HbR and HbO in optic window.

$$\Delta A_{760} = (\alpha_{760\,HbR}\Delta[HbR] + \alpha_{760\,HbO}\Delta[HbO])\,dB \quad (1-9)$$

$$\Delta A_{880} = (\alpha_{880\,HbR}\Delta[HbR] + \alpha_{880\,HbR}\Delta[HbO])\,dB \quad (1-10)$$

Then detected light signal would be like figure 1-3, if use high (peak) point and low (valley) point of signal as A_1, A2 respectively at equation (1-8), equation (1-9, 10) become below

$$\Delta A_{760} = (\alpha_{760\,HbR}[HbR] + \alpha_{760HbO}[HbO])\,dB \quad (1-11)$$

$$\Delta A_{880} = (\alpha_{880\,HbR}[HbR] + \alpha_{880\,HbR}[HbO])\,dB \quad (1-12)$$

Because [HbR], [HbO] at valley is approximately zero. [7]
The ratio of the arterial transmittance measured at two wavelength, a ratio R_{OS} that is called ratio of ratio can be calculated such that

$$R_{OS} = \frac{\Delta A_{760}}{\Delta A_{880}} \quad (1-13)$$

Conventional pulse oximetry assume that ROS and SpO2 have linear correlation like equation (1−14) and make look up table.[8]

$$S_pO_2 = a\ R_{OS} + b \quad (1-14)$$

1.2.2.3 Calibration of Pulse Oximeter

1.2.2.3.1 In vivo Calibration

In vivo calibration was until 1993 the only method used to calibrate pulse oximeters. [9] In vivo calibration typically takes place in a hospital environment using informed and consenting, non−smoking, healthy volunteers as human test subjects. Subjects are fitted with an indwelling arterial cannula placed in the radial artery. An initial arterial blood sample is taken and tested to ensure that only normal adult hemoglobin is present and that each subject's background levels of carboxyhaemoglobin and methaemoglobin are within normal limits. Typical values are MetHb < 1% and 1% < COHb < 2% [9] A CO−oximeter is used to determine the oxygen saturation of the blood samples precisely. The subjects breathe air or oxygen−enriched air until their arterial blood samples show 100% saturation. The subjects' arterial oxygen saturation is gradually and incrementally reduced by replacing the oxygen in their breathing gas with nitrogen, and pausing at each step to

allow time to equilibrate. When the device under test indicates a stable reading, an arterial sample is immediately taken and analyzed by the CO-oximeter. The data from each device are plotted against each other to yield a graph with oxygen saturation on the vertical axis and ratio of absorption at two wavelengths on the horizontal axis. A lookup table is then constructed to perform an exact mapping of the R_{OS} readings from the device under test to the corresponding S_aO_2 level, or, a transform equation is constructed that generates a best fit to the plotted graph. This process must be repeated for every LED wavelength combination that the manufacturer intends to use in their probes.

There are several reasons why in vivo calibration is unsatisfactory. The principal reason is that because it is unsafe to desaturate a human test subject below 85% (due to the aforementioned risk of hypoxic brain damage), the data that result from in vivo calibration pertain only to high oxygen saturations-where the need to ascertain accurate oxygen saturation reading.[5]

1.2.2.3.2 In vitro Calibration

In vitro calibration methods can be divided into those that use blood or hemoglobin solutions and those that do not. Methods that do not use blood or hemoglobin solutions can generally provide only one reference saturation point, which limits their utility. Though the appeal of a blood free device is such that several attempts have been published for a pragmatic example-the consensus however, is that versatile in vitro methods require a blood or hemoglobin solution [10] Several blood-based in vitro techniques have been described in the literature and in patents, ranging in complexity from Yount' s wedge-based technique to the comprehensive system described by

Reynolds et al.[10]

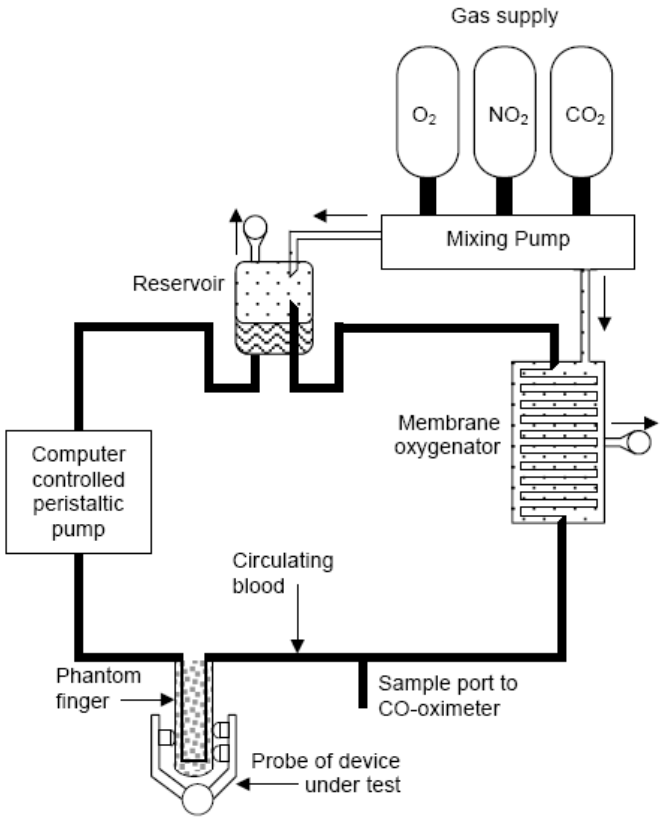

Figure 1-4. Apparatus for in vitro calibration of pulse oximetry [5]

The system described by Reynolds et al. is depicted in Figure 1-4. It serves as a good example of the tasks and components involved.

The system uses whole blood to which the anticoagulant heparin has been added. A computer controlled peristaltic pump circulates the blood around a closed loop with minimum damage to the erythrocytes, mimicking the pulsatile blood flow of the arteries. A gas-mixing pump provides a mixture of O_2, N_2 and CO_2, in user defined proportions. The CO_2 is necessary to maintain the correct pH and realistic carbon dioxide partial

pressure. Gas diffuses into and out of the blood through an oxygen membrane, which provides a large permeable interface area with gas on one side and a thin film of blood on the other, mimicking the alveolar function of the lungs. The probe of the pulse oximeter under test is attached to a phantom finger in which the blood is circulating. A sample port provides an extraction point for blood samples, which are subsequently analyzed by a CO-oximeter. The computer, using parameters fed-back from a second, modified pulse oximeter, varies and controls the gas mixture and rate of peristaltic displacement, to simulate the desired heart rate and arterial oxygen saturation.

The construction of the phantom finger, to which the probe of the device under test is attached, is an important factor. The phantom should possess similar absorptive and scattering properties to a real finger and in addition, should exhibit a similar variance in volume to a real finger, when exposed to the artificial pulse. [5]

1.2.3 Functional Near Infrared Spectroscopy

1.2.3.1 Brief Functional NIRS Event Overview

As portrayed in figure 1-5 near-infrared light is applied in contact with, and perpendicular to the scalp. The NIR light enters the epidermis and after only a few millimeters becomes highly diffuse due to multiple scattering events due to the refractive index mismatches mostly between extracellular and intracellular boundaries [11]. Scatter will occur wherever there is a change in refractive index. The further NIR light has to travel in a highly scattering medium, the greater the angle of scattering. From diffusion theory, the more scattering particles there are in a medium the greater the probability that the light will be backscattered – that is that the light travels a net direction of ~180 in reference to the light source injection [12]. Thus the light is said to travel a random walk path but in a pseudo-arc or banana-like path with decreased photonic emergence from the scalp a few centimeters from the source

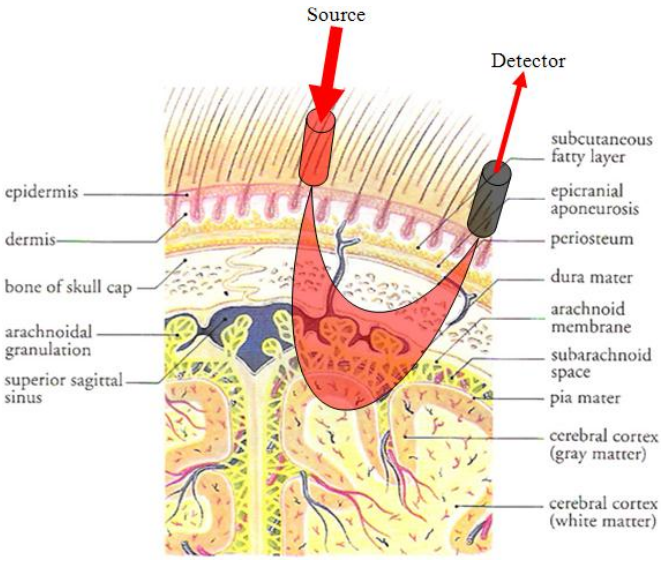

Figure 1-5. Conceptual arc-like NIR light propagation in the human head penetration to the cerebral cortex. [15]

A detector placed approximately 3cm from the source can collected sufficient photons (~10^6–10^7 loss – so 1 out of a million photons) which have travelled through the cerebral cortex – the outer layer of the brain. It can be claimed that these photons have travelled into the cerebral cortex since photonic penetration into the brain or photonic depth is proportional to the distance between the source and detector, with ~3cm being the standard inter–optode (IOS) distance for cerebral interrogation.

In other words, in general NIR light emerging <1.5cm from the source cannot penetrated deep enough to reach the brain [13] but only interrogates the superficial layers (meninges, skin, bone etc.). It is principally the changes in NIR light absorption that provides the crucial information about the functional activity of that localized tissue (which accounts for 20% of light attenuation [14]). With a functional event, such as movement of a limb, the brain tissue responsible for controlling that event becomes more metabolically active, and a neurovascular process ensues due to increased metabolism. A focal/regional increase in cerebral blood volume (rCBV), cerebral blood flow (rCBF), and the cerebral metabolic rate of oxygen consumption ($rCMRO_2$) pseudo–superimpose (time evolutions differ) to give a distinct pattern of hemodynamics. This induces a distinct pattern in NIR light absorption which is wavelength–dependent for the two main hemoglobin molecule states: oxygenated (HbO_2) and deoxygenated (HbR). Thus, to resolve changes in HbO_2 and HbR the spectroscopes require at least 2 wavelengths of light (to solve the simultaneous equations of the modified Beer–Lambert Law described earlier). Specifically, NIR light below the isosbestic point (800nm for HbR and HbO2 absorption spectra) for HbO2 and HbR is more sensitive to changes in HbR than HbO2. Similarly NIR light above 800nm is more sensitive to HbO2 concentration changes

than HbR. Thus for example more absorption of the <800nm light source indicates a more distinct change of HbR concentration in the localized tissue. This process will be described in more detail in the following sections, such as the importance of selecting the correct wavelength pair.[15]

1.2.3.2 Functional Cortical Map

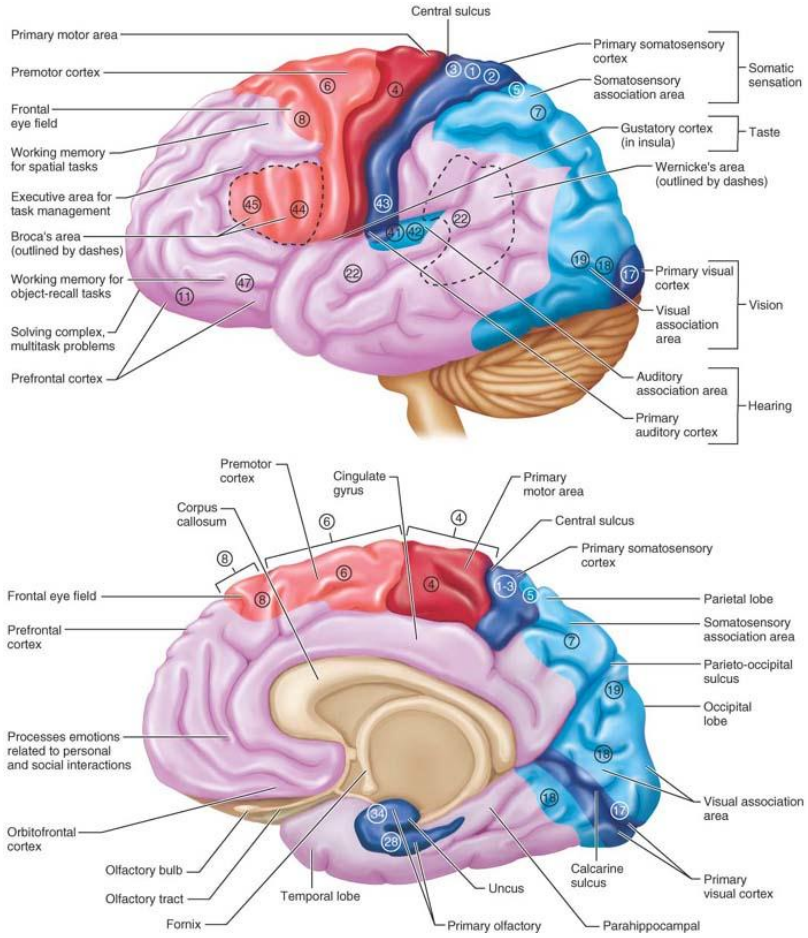

Figure 1-6. Cerebral cortex – functional and structural map [15]

1.2.3.3 Three Main Techniques of fNIRS Instrument

1.2.3.3.1 Continuous Wave NIRS

CWNIRS is perhaps the least demanding method in terms of hardware, optics, and speed of data processing, and it has the greatest potential for miniaturization, even to a wireless system.[16] Only changes in light intensity (attenuation) are measured with this technique, whereby the light sources are turned on continuously, or modulated at low frequencies – a few kHz. At present they are the most common NIRS imager[17] due perhaps to the flexibility of the modality, although the technique can only resolve qualitative information on the changes in concentration of the various chromophore, e.g. oxy hemoglobin. Quantitative measures are impossible with this technique due to the highly scattering (mostly elastic) nature of biological tissue whereby the path length of the light is extended to typically six times the distance between the source and detector. This term, the differential path length factor (DPF) cannot be measured directly in CWNIRS and so tabulated values are used for typical tissue models, e.g. the adult head, and different wavelengths (i.e. the DPF is tissue– and wavelength dependent). Nevertheless, CWNIRS is suitable for functional studies where concentration changes in chromophores are sufficient for determining functional activity. [18] For quantitative measurements where absolute levels are required such as in neonatal cerebral oxygenation monitoring, two principle methods can be used – time resolved– and phase resolved spectroscopy. [12]

1.2.3.3.2 Time–Resolved (Time domain) Spectroscopy

In order to determine the mean optical path length (OL) of

light travelling through tissue, time-resolved spectroscopy (TRS) delivers a short pulse of light (~2ps-5ps) which can then be detected with a suitably fast detector. The tissue scattering these photons cause the delta pulse to broaden, such that a histogram of arrival times of photons is developed. The time it takes for photons to traverse the tissue is called the time-of-flight (TOF), and is the time difference between the incident light pulse peak-intensity and the peak of the transmitted light temporal point spread.

1.2.3.3.3 Phase-Resolved (Frequency domain) Spectroscopy

Instead of measuring time of flight directly, a frequency based temporal calculation of the propagation delay of photons due to scatter is possible by assessing the phase shift of a light source whose intensity is modulated in the range of hundreds of MHz. [19] The absorption due to the tissue can also be measured by an assessment of the AC and DC attenuation of the detected light intensities (at the intensity modulation frequency).[15]

1.2.3.4 fNIRS Application Areas

fNIRS can be used at i) physiological measures based on fNIR to predict changes in cognitive workload during a complex cognitive task such as control of airplane. ii) brain Function monitor for intra-operative awareness during surgery iii) pain assessment iv) brain computer interface etc. [20]

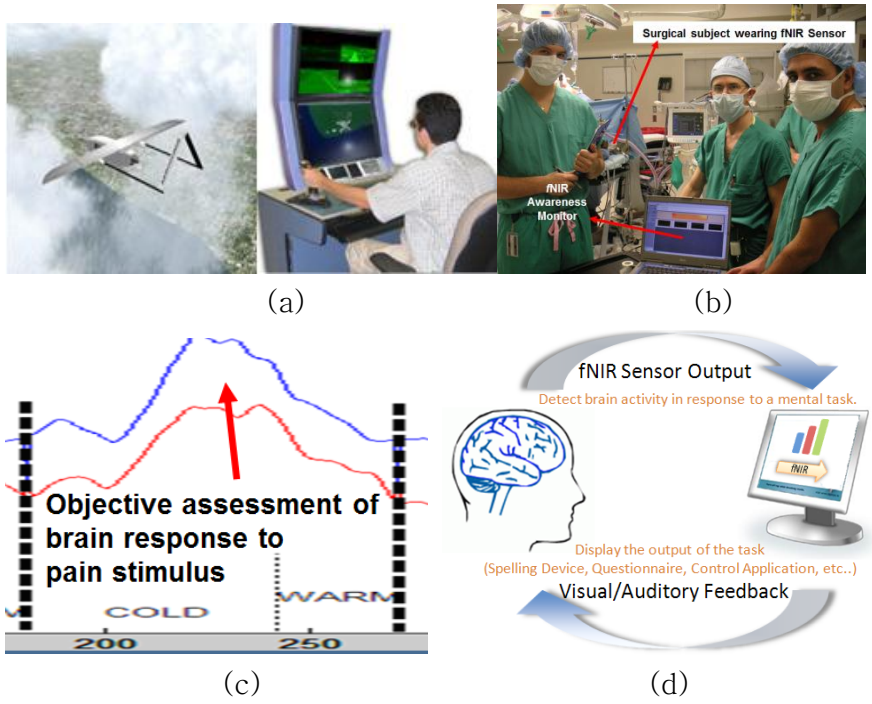

Figure 1-7. fNIRS application areas (a) Human performance assessment using fNIRS (b) Depth of anesthesia monitoring (c) Pain assessment (d) Brain computer interface

Chapter 2. Development of Power LED-PIN PD Based Biomedical Signal Monitoring System

2.1 High Power Output Light Source with Two Different IR Wavelengths (Dies)

2.1.1 Review of Two types of Emitter

LD and LED are only possible IR light emitters for non-intrusive optic biomedical signal monitoring system. LED has good linear properties between current and output. Also it is relatively cheap and easy to control. So LED is widely used at conventional pulse oximeter. However, the main drawback of LED is relatively weak output compare with LD. So LD is used as light source when high light output is needed such as conventional optic fiber-LD based fNIRS. Simultaneously, LD has many drawbacks such as complex, expensive LD driver and non-linearity. (Figure 2-1, Table 2-1) So LD is not good for portable and daily biomedical signal monitoring system. And though LED has lower output than LD, LED can emit enough power output by applying peak forward current modulation. It will be explained 2.1.3 in detail. For these reason, we decided to use LED as emitter.

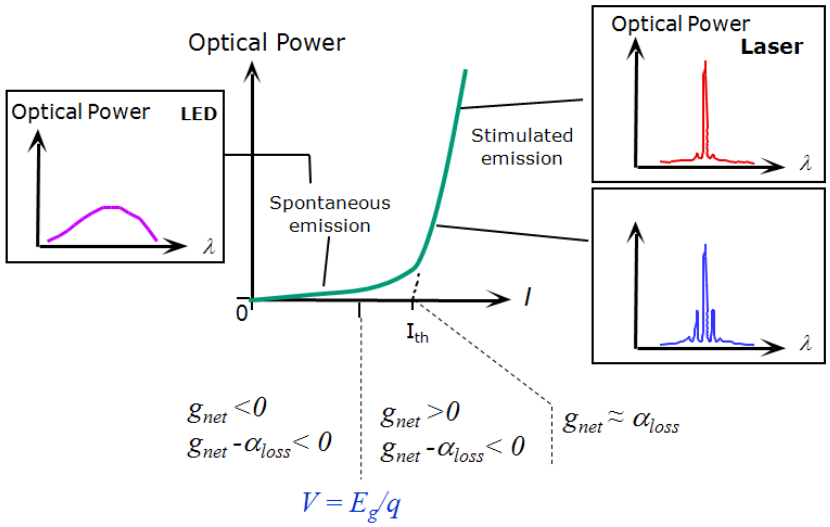

Figure 2-1. Light output power, optical spectra, and net gain as a function of current.

Table 2-1. Comparison of LED and LD

	LED	LD
Principle of light formation	Spontaneous Emission	Stimulated Emission
Radiation Pattern	No Directionality	Has Directionality
Spectrum BW	40nm	0.01nm(mono mode)
Response Time	nsec	Psec
Current- Output	Linear Analog transmission	Non-linear Digital transmission
Driver	Relatively Simple and Cheap	Complex, Expensive. (Temperature compensation Circuit required)

2.1.2 Power LED with Two Different IR Wavelengths

2.1.2.1 LED Design

There is no conventional power LED with two different IR wavelengths so I used custom made LED (OD-1894, Opto diode corp.). This LED has 760nm, 880nm dies. The specification of each dies described at table 2-2. 880nm dies are same with die of OD880F (Opto diode corp.) and 760nm dies are custom made for this LED by Opto diode corp. For the same intensity of each dies, four 760nm dies arranged in the package per one 880nm in one package.

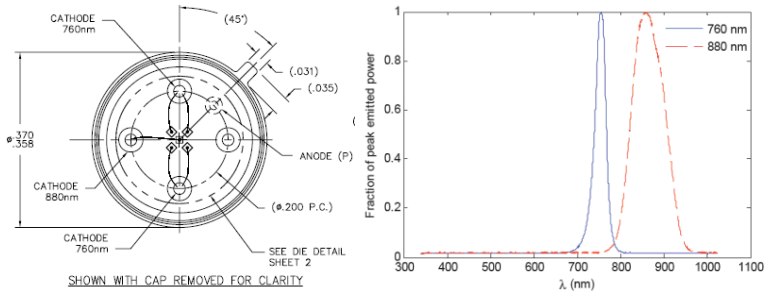

(a) (b)

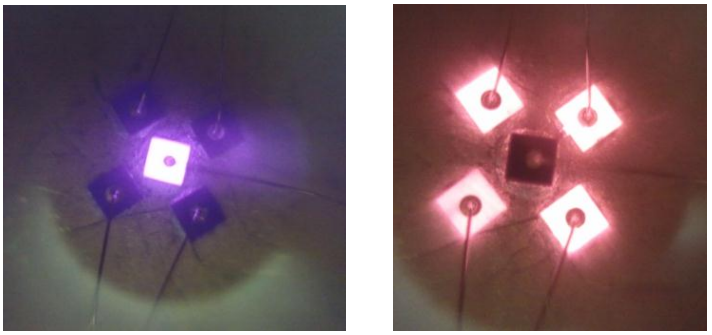

880nm 760nm

(c)

Figure 2-2. (a) OD-1894 schematic (b) LED emission spectra at 30mA (c) Distribution of LED chips (dies)

Table 2-2. OD-1894 specifications of each LED chips

760nm LED (Per Connection)

PARAMETERS	Test Conditions	MIN	TYP	MAX	UNITS
Total Power Output, PO	IF = 100mA	10	15		mW
Peak Emission Wavelength, λP	IF = 20mA		760		nm
Spectral BW at 50%, Δλ			30		Nm
Forward Voltage, VF			1.50	1.90	Volts
Reverse Breakdown Voltage, VR	IR = 10uA	5			Volts

880nm LED

PARAMETERS	Test Conditions	MIN	TYP	MAX	UNITS
Total Power Output, PO	IF = 100mA	10	15		mW
Peak Emission Wavelength, λP	IF = 20mA		880	900	Nm
Spectral BW at 50%, Δλ			80		Nm
Forward Voltage, VF	IF = 100mA		1.55	1.90	Volts
Reverse Breakdown Voltage, VR	IR = 10uA	5	30		Volts

2.1.2.2 LED Control using Peak Forward Current Modulation

As duty cycle decreased, LED can endure higher current. Because forward current and power output of LED die has linear correlation, power output can be higher as duty cycle decreased. (Figure 2-3) According to the paper, LED output need to be higher than 25mW for penetrating skull bone.[21, 22] 880 nm die of OD-1894 emits about 100mW power output under 100us, 100Hz (1% Duty cycle), 1A forward current (maximum value) condition and 760nm dies of OD-1894 emit about 40mW power output under 100us, 100Hz (1% Duty cycle), 400mA forward current (maximum value) condition. Output power of each dies was enough for power LED - PIN PD based biomedical signal monitoring system such as fNIRS or unconstrained pulse oximeter.

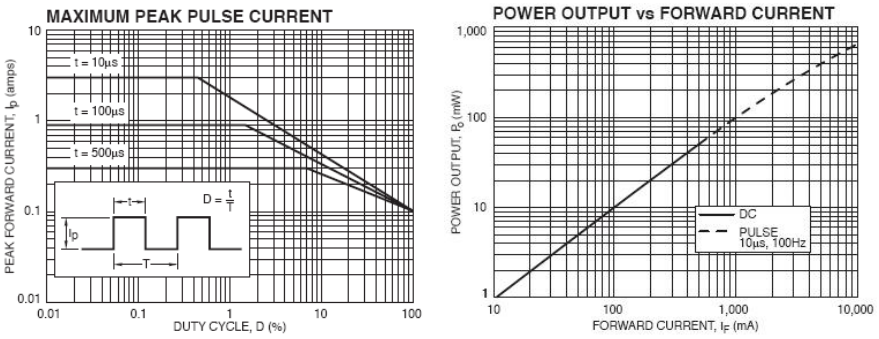

(a) (b)

Figure 2-3. LED modulation specification plot(OD-880) (a) Maximum peak pulse current- duty cycle (b) Power output - forward current

2.1.3 Schematics of LED Driver for each dies

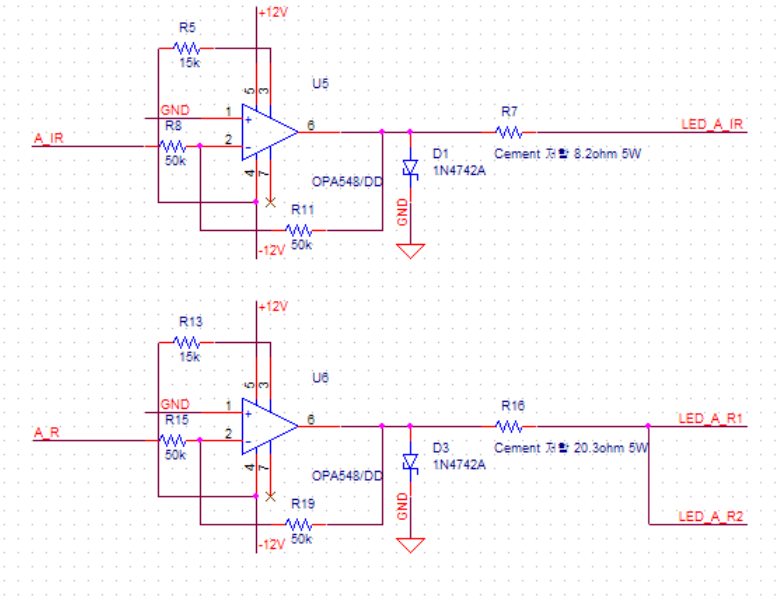

Figure 2-4. LED driver for each dies

760nm, 880nm dies need to be controlled separately and operation current have to be more than 400mA and 1A respectively when LED operated under peak forward modulation. So we used OPA548 (5A peak current, Texas instrument) as driver op-amp and AD558 (8-bit DAC, Analog Devices) for voltage control. We used MUX (ADG508 or ADG5436, Analog devices) for separate operation of each die. Capacity of current restriction resister should have more than 10W capacity (at peak operation more than 5W). For the protection of the LED, Zener diodes (1N4742) are used and OPA548 are driven current restriction mode. DAC and MUX are controlled by MCU.

2.1.4 Adaptive Light Intensity Control

According to the site that power LED – PIN PD Based biomedical signal monitoring System is applied, the environment (such as contacted area, thickness of substance between sensor and skin etc.) is changed dramatically. Because of this, the signal saturation or very weak signal acquisition from detector can be happened. So we devised adaptive light intensity control technique. Similar idea has been existed[23] and we modified the idea more precisely. We decided optimal signal range. If detected signals exceed maximum limit of optimal signal range, light intensity go lower. If signal is lower than minimum limit of optimal signal range, light intensity go higher. MCU operates these comparison operations and controls LED through DAC.

```
function adaptive light control(sig_min, sig_max)
{
        get_signal()   // collect IR, R data
// increase light intensity when signal weaker than signal minimum range

if ( (IR_data < Sig_min) & (IR_int_idx < 250) )
IR_int_idx = IR_int_idx + 1;

if ( (R_data < Sig_min) & (R_int_idx < 250) )
R_int_idx = R_int_idx + 1;

// decrease light intensity for preventing signal saturation

if ( (IR_data > Sig_max) & (IR_int_idx > 36) )
IR_int_idx = IR_int_idx - 1;

if ( (R_data > Sig_max) & (R_int_idx > 36) )
R_int_idx = R_int_idx - 1;

}
```

2.2 High Sensitive Photo Detector within IR Range

2.2.1 Review of Four types of Photo Detectors

As a detector, four types of photo detector can be used i.e. PMT, APD, PIN PD and PN PD. PMT is extremely sensitive detectors of light and being widely used in medical diagnostic fields including blood tests, medical imaging. APD are alternatives to photomultipliers; however, photomultipliers are uniquely well-suited for applications requiring low-noise, high-sensitivity detection of light that is imperfectly collimated. However PMT needs too much voltage (generally more than 200VDC) to operate portably and volume of PMT is relatively huge so that hard to be embedded in the portable device. (Figure 2-5 (a)) APD is small enough and most sensitive photo detector among solid state photo detectors, but it also needs high voltage(generally more than 100VDC) to have high gain and complex driver (such as temperature compensation module) for keeping linearity.(Figure 2-5 (b))

PN PD and PIN PD are relatively easy to control. A PIN PD is a PN PD with an intrinsic region between a P and N regions. A wide, lightly doped intrinsic region make PIN PD have much better sensitivity and lower capacitance than PN PD so PIN PD perform faster operation. Even though PIN PD need reverse voltage, the optimum value of reverse voltage is relatively low (generally around 10V) and safe as long as it with proper shielding. So it is decided to use PIN PD as photo detector for portable and daily-applied optical biomedical signal monitoring system.

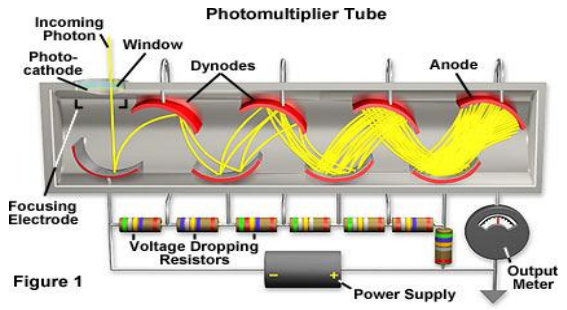

(a)

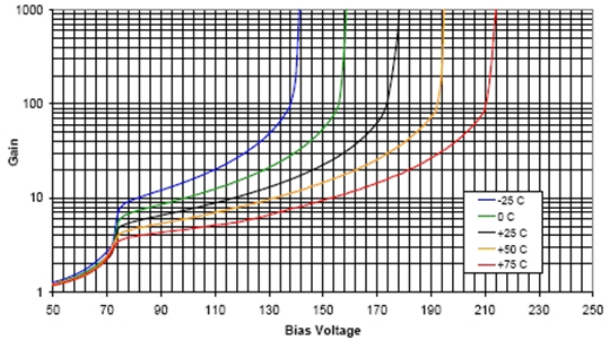

(b)

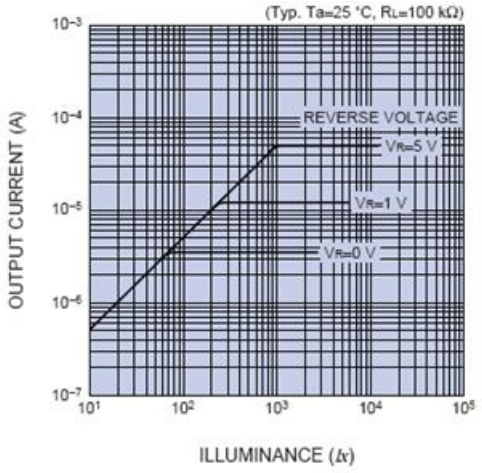

(c)

Figure 2-5. (a) PMT (b) APD reverse voltage – gain plot (SAE230NS series, Laser Components Inc.) (c) PIN diode illuminance vs. Output current characteristics

2.2.2 Schematic of PIN diode Circuit

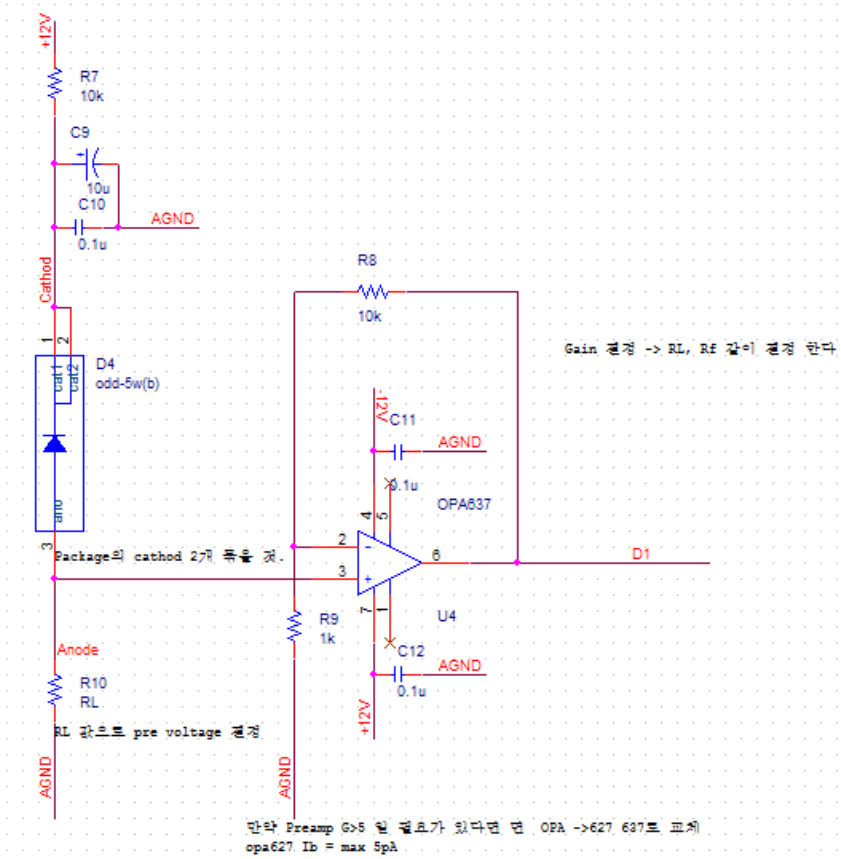

Figure 2-6. Schematic of PIN diode Circuit

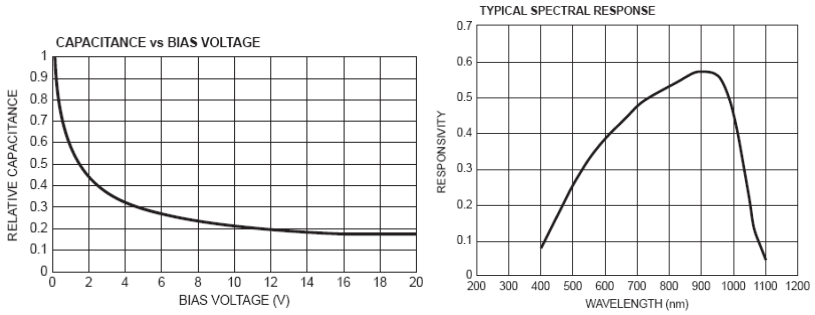

(a) (b)

Figure 2-7. ODD-5WB Characteristics. (a) Capacitance vs. Bias Voltage. (b) Typical spectral response.

In this paper, ODD-5WB (Opto diode Corp.) is used as

detector. PIN diode needs reverse bias voltage for high sensitivity as shown in figure 2-6. Bias voltage was 12V. Load resistor R_L, pre-amp gain need to be optimized according to light intensity.

Chapter 3. Design of Auto Light Intensity Controlled Reflection Type Pulse Oximeter

3.1 Modified Beer-Lambert Law with changing light

With changing light intensity, equation (1-1, 4) becomes equation (3-1). Here k is proportion of changing light intensity.

$$I = k\, I_0\, e^{-(\alpha c d\beta + G)} \quad (I_0 \rightarrow k \text{ times}) \qquad (3-1)$$

$$A = \ln(I_0/I) = \alpha c d\beta + G - \ln(k) \qquad (3-2)$$

$$\begin{aligned} \Delta A &= A_2 - A_1 \\ &= (\alpha c_2 d\beta + G - \ln(k)) - (\alpha c_1 d\beta + G - \ln(k)) \\ &= \alpha (c_2 - c_1) d\beta = \alpha \Delta c d\beta \\ &= (\alpha HbO \Delta [HbO] + \alpha HbR \Delta [HbR])\, d\beta \end{aligned} \qquad (3-3)$$

Equation (3-3) becomes same with equation (1-8). It shows that the light changing does not effect on conventional optical arterial blood oxygen saturation calculation. Effect of substance between sensor and skin are also eliminated through assuming it as part of B and G in the equation. As a result, it becomes possible to use auto adaptive light intensity control technique.

3.2 System Overview

For transplantation in the chair or bed, the pulse oximetry system needs to be reflection type not penetration type as conventional pulse oximetry. With the adaptive light intensity control technique that is explained in 2.1.4, robust reflection type pulse oximeter can be realized. For higher light intensity for overcoming thick cloths or bed cover between skin and sensor, we arranged one PIN PD at the center of sensor and three power LEDs around detector with 1cm distance from center to center. (Figure 3-1)[24] Overall system block diagram is figure 3-2. MCU execute LED control through DAC and MUX, data transmission to the PC by serial communication using blue tooth. Signal separation between 760, 880nm is done with TDM (Time Division Multiplex) i.e. each die turned on and signal sampled rotationally. PC execute digital filtering, peak detection algorithm for calculation S_pO_2 and display signal including wave form, high and low peak, heart rate.(Figure 3-3) For peak detection, we used CGS algorithm that is not yet published. CGS algorithm detect peak of PPG signal very well and is stubborn to noise.[25]

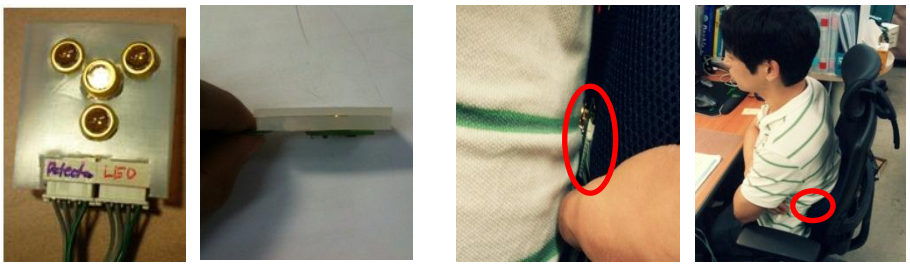

(a) (b)

Figure 3-1. (a) Reflection type pulse oximeter (2.8x3.0x1.0 cm) (b) Signal acquisition during sitting a chair.

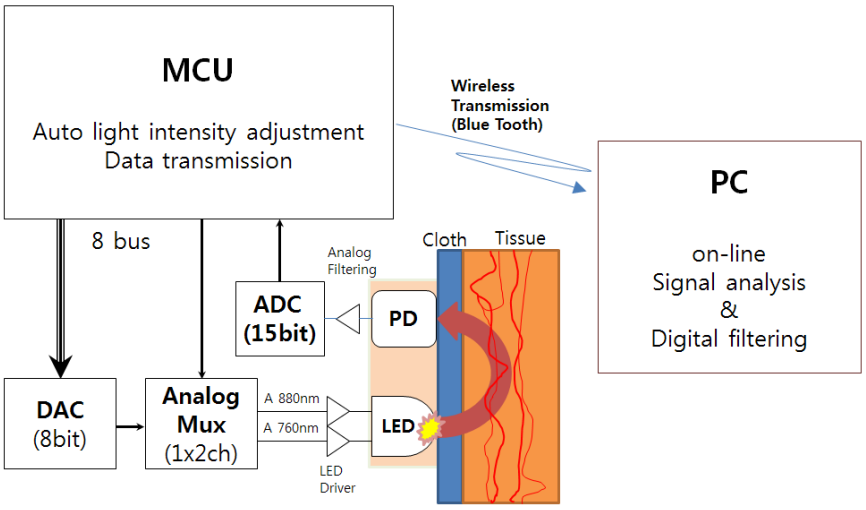

Figure 3-2. Block diagram of auto light intensity controlled reflection type pulse oximeter

3.3 Results

(a)

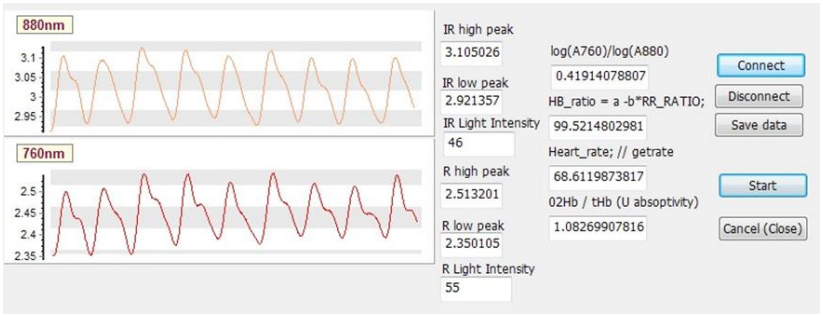

(b)

Figure 3-3. (a) Signal from covered finger with cotton dress (0.36mm) (b) Signal from covered back with 2 layer of dress (0.66mm)

As it is shown at the Figure 3-3, the transmitted data from pulse oximeter is displayed at the viewer. Displayed graph at the left side is 5Hz Low pass filtered. Using CGS algorithm, high and low peak of 880nm (IR) and 760nm(R) are picked respectively. (*IR high peak, IR low peak, R high peak, R low peak*) According to changing of each wavelength 's intensity at the board side, light intensity data are transmitted to PC and display as well. (*IR Light Intensity, R Light Intensity*) *log(A760)/log(A880)* means Ratio of ratio that explained at the chapter 1.2.1. Also, SpO2 can be derived from Ratio of ratio. At this experiment, the SpO2 doesn't exact as I explained at the Chapter 1.2.2.3 but I shows the possibility of real time SpO2

display as long as there was the calibration that is mentioned at the Chapter 1.2.2.3. The heart rate is also able to be counted through counting high peak of each wave length’ s signal.

3.4 Discussions

The determination of arterial oxygen saturation by the technique of pulse oximetry requires calibration of the device either in vivo which requires a clinical or in vitro which requires obtaining and artificially oxygenating whole blood; both are beyond the purview of this research. However, this research shows the possibility of non-intrusive pulse oximeter that can detect oxygen saturation under various environments. This new type of oximeter can be used not only by transplanting in the chair or bed but also as wearable form.

The key feature of this pulse oximeter is that the light intensity is adjusted adaptively according to its environment. If substances between light emitter and detector become thicker, the light intensity becomes stronger. On the other hand, if substances between light emitter and detector become thinner, the light intensity becomes weaker.

However, for the precise measurement of the oxygen saturation, advanced filtering techniques are needed to apply such as adaptive filtering. According to literature, elimination of motion artifact can be improved by using Kalman filtering technique and advanced adaptive filtering.

Chapter 4. Design of the Multichannel fNIRS Instrument

4.1 System Overview

Figure 4-2 is overall system block diagram of the multichannel fNIRS instrument. The system has 4 light emitters, 10 main detectors, 4 reference detectors, and 3-axis accelerometer and all data sampled at 100Hz.

MCU execute DAC control (by 8 control bit bus), 8ch and 16ch analog MUX control(by 3 control bits, 4 control bits, respectively), accelerometer axis selection(by 2 control bits), data acquisition from 15 bit ADC through SPI communication, internal ADC(10bit) signal from accelerometer and serial communication with PC through Bluetooth®. D0~D9 and Da~Dd stand for main and reference detectors respectively. Specifications of each single detector are similar but pre-amp gain of main detector is higher than reference detector. The reason why we made like this is the purpose of reference detector that would be arranged near LED than main detector is removing PPG signal of superficial skin.

For versatile use of this module, we make LED and detector module one by one so it can be arranged freely. According as desired site of head, LED and detector arrangement would be decided. (Figure 4-2, Figure 4-3) Versatile use electrode arrangement (Figure 4-3 (b)) can be applied at frontal lobe widely. It also can be used at motor cortex or visual cortex but the main problem is hair that blocks light almost completely even with thin thickness. So we designed motor and visual cortex use electrode arrangement. (Figure 4-3 (c, d, e)) The distance between F1 and F2 same with O1 and O2 so visual cortex use electrode arrangement can be used at Frontal lobe.

The process of installation is shown at figure 4-4. This works do not take for a long time and detect hemodynamics of the site that the pads attached. Figure 4-5 is viewer of this module. This display each signal of detector channels (10 channels of main detectors and 4 channels of reference detectors) and accelerometer on-line, and save the data for off-line data analysis.

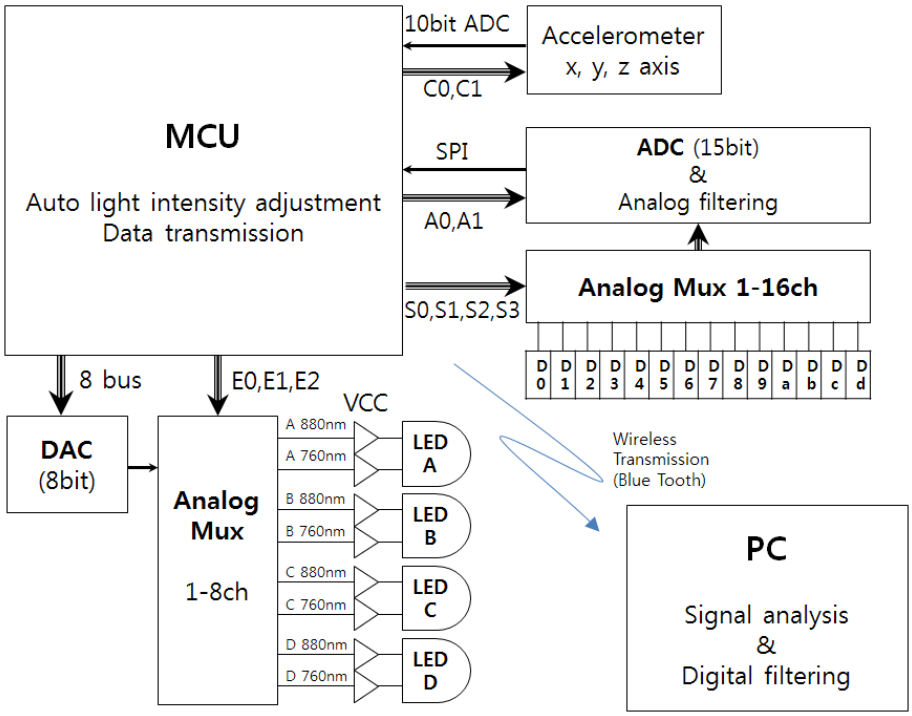

Figure 4-1. Block diagram of multichannel fNIRS instrument

(a) (b) (c)

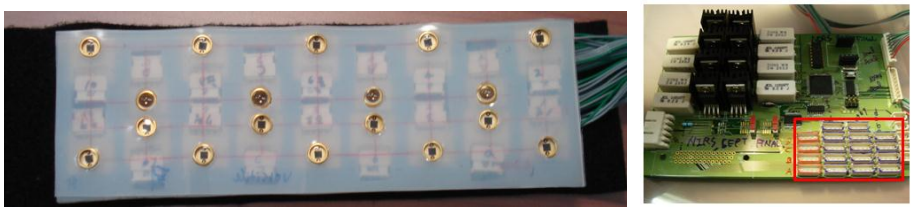

(d) (e)

Figure 4-2. Actual image of (a) LED (1.5x1.5 cm2) (b) PIN PD (1.8x1.8 cm2) (c) Accelerometer (2.3x1.9 cm2) (d) Versatile used fNIRS pad. (e)Control board and connector for LED and detector (red square)

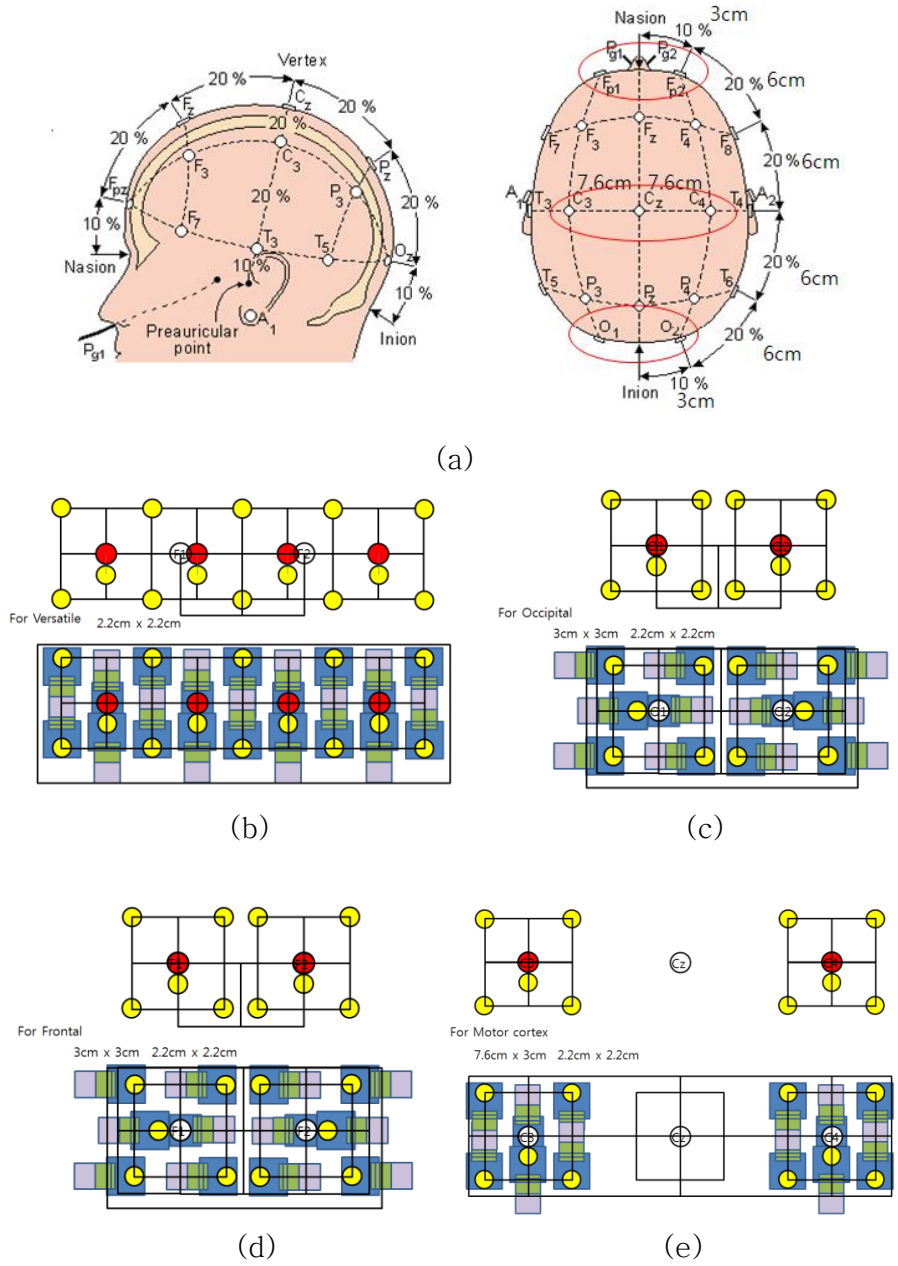

Figure 4-3. (a) International 10-20 system. Electrode arrangement of (b) Versatile use (c) Occipital site (d) Frontal (e) Motor cortex (Red : LED, Yellow : PIN PD)

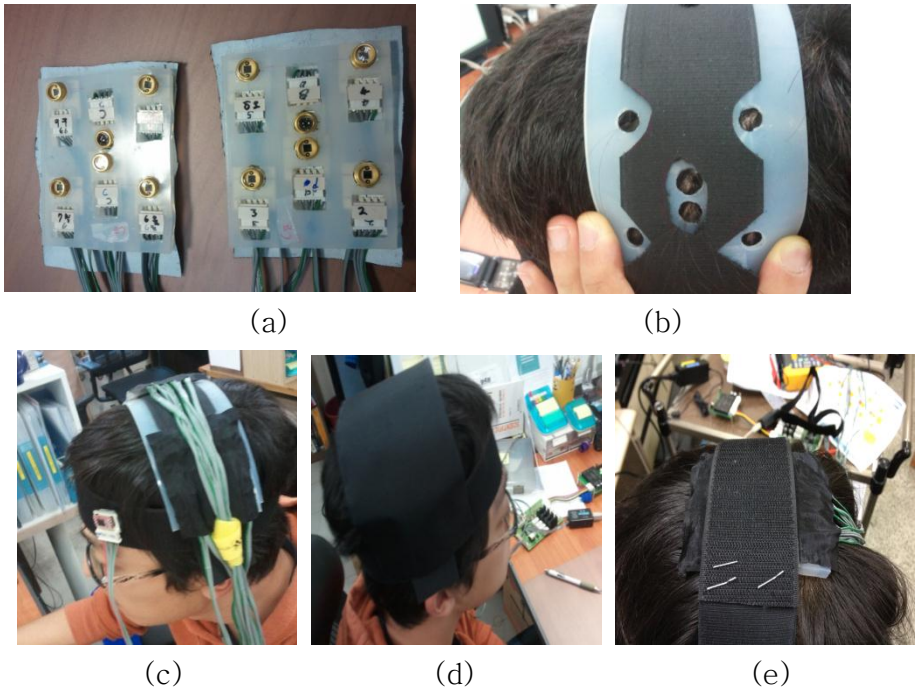

Figure 4-4. Installation of fNIRS pad for motor cortex (a) Actual image of fNIRS pads for motor cortex (b) Removing hair (c) Applying pads at C3 and C4 (d) Fixing the pads. (e) Applying pad at the Cz with same way

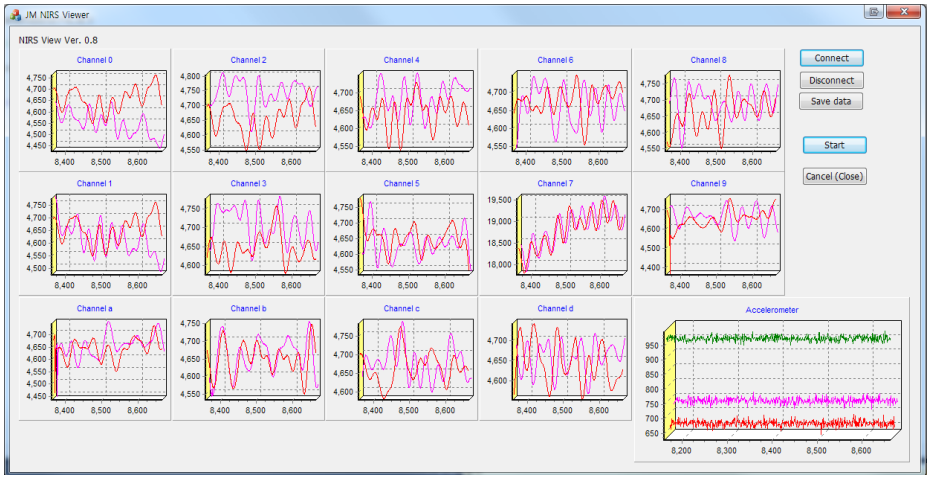

Figure 4-5. fNIRS signal viewer

4.2 Results

Various evaluation methods were tried for evaluating this fNIRS module. All after, I found that detection of motor cortex blood volume change is the best protocol to evaluate fNIRS.

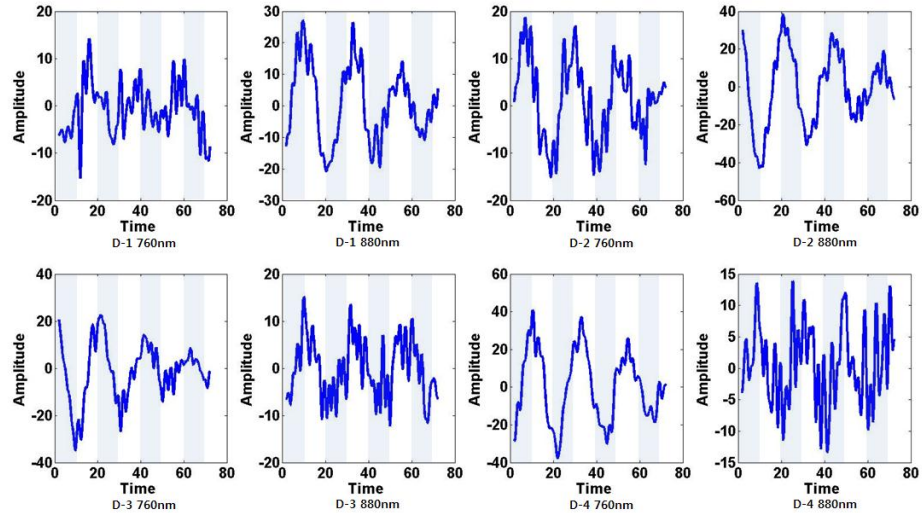

Subject 1

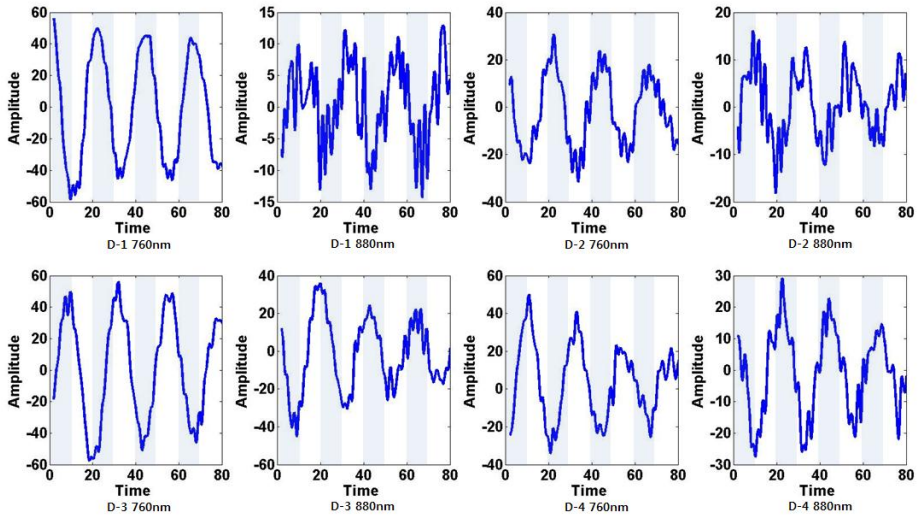

Subject 2

Figure 4-6. Signal waveforms of each site. (Blue: 10s Resting, White: 10s tapping. Unit of x-axis is second.)

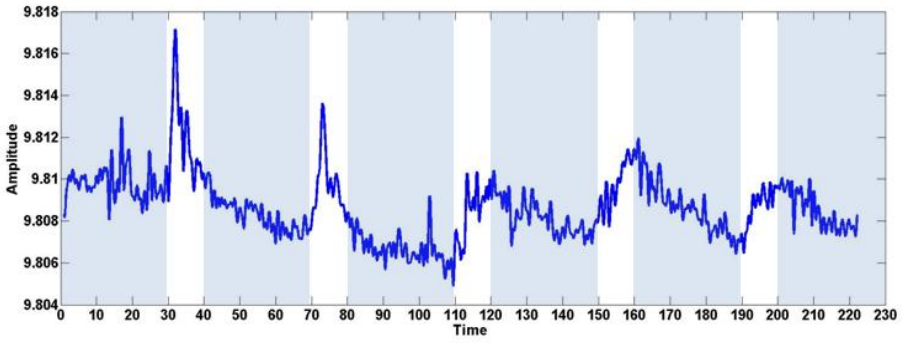

880nm

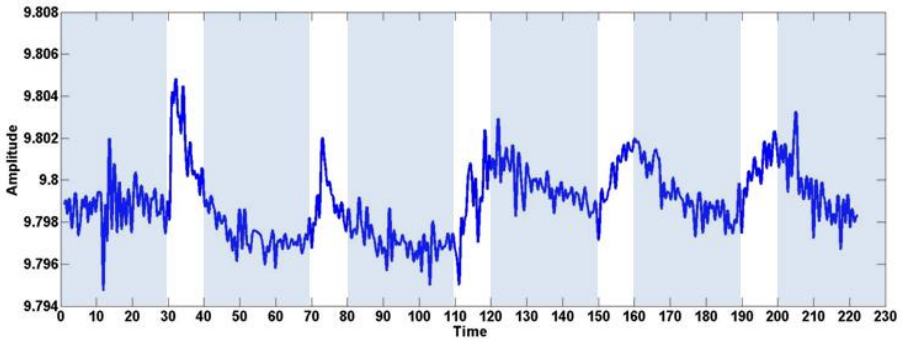

760nm

Figure 4-7. Signal waveforms of Cz during Finger Tapping (Blue: 30s Resting, White: 10s tapping. Unit of x-axis is second.)

There are two protocols there. First protocol is the repeated movement of 10 seconds rest and 10 seconds finger movement. Second is the repeated movement of 30 seconds rest and 10 seconds finger movement. Figure.4-6 is signal from each site. Each signal was band pass filtered from 0.1Hz to 3Hz. Signal wave form synchronizes with each movement of finger. Trend of each signal changes synchronized with each tasks. Likewise, Signal sync with task is also found in result of second protocol. (Figure.4-7) Because signal draft of second protocol experiment was enough to classify between tapping and resting zone, the signal was filtered with 3Hz low pass filter.

4.3 Discussions

I have done various methods for evaluation this module. For example, frontal lobe hemodynamics detection during mental calculation or hemodynamics changes before and after muscle movement. However, the best way for evaluation NIRS module is motor cortex hemoglobin detection during limb movement. The result shows that hemodynamics synchronizes with movement of finger tipping. However, the research that finds the exact meaning of this should be operated on the top of my research. Also, like reflection type pulse oximeter, if there was calibration that shows the relation between light intensity and absolute value of hemodynamics, finding quantitative meaning of signal will become easier. Moreover, advanced filtering technique can be applied by using accelerometer data. In this system, the signal processing is operated at the PC so real time processing can be done easily without using DSP. There is lots of BCI system using EEG signal that is wearable but few NIRS BCI system is ongoing at the moment. The reason is that conventional NIRS systems use LD as light source and APD as detector so the system volume is too big. If advanced filtering technique applied at this system, robust wearable NIRS system will be realized.

Chapter 5. Conclusions

In this thesis, I focused on describing optical biomedical signal acquisition system that based on power LED and PIN PD. The purpose of developing this system is making unconstraint and portable optical biomedical signal acquisition applications such as pulse oximeter embedded in furniture or portable NIRS module.

Pulse oximeter needs to be embedded in furniture such as chair or bed for unconstrained oxygen saturation monitoring in daily life. For this transplantation, the pulse oximeter was designed as reflection type rather than conventional penetration type. Also, I controlled this pulse oximeter with auto-adjustable light intensity control technique that described in chapter 2.1.4. This technique is essential in this embedded and reflection type pulse oximeter because there should be much more environment variety than penetration type one such as substance and distance between light emitter and detector. Signal saturation or weak signal can be prevented with auto-adjustable light intensity control technique.

The PPG signals of each wavelength were detected well as shown figure 3-3. Based on signals, ratio of ratio and pulse rate also can be derived.

Conventional NIRS applications generally use laser diode as light emitter and avalanche photo diode as light detector. However, for the portable NIRS module, laser diode (LD) and avalanche photo diode (APD) is not suitable because of these large volumes of control module and unsafety. The solution was using power LED and PIN diode. There are many shortcomings of power LED and PIN diode compare with LD and APD. Power LED has lower light intensity and wider spectrum band width than LD. PIN diode also has lower sensitivity than APD. For these reasons, the spatial resolution of power LED and PIN

diode based is lower than LD and APD based. At the same time, continuous wave NIRS is only possible to be used. Despite of these defects, many NIRS group uses power LED and PIN based technique because of its simplicity and safety.

In the above experiment, I added auto light intensity control technique on the conventional power LED and PIN diode based NIRS and added reference detector for removing superficial artifacts and simultaneous sampled accelerometer for advanced filtering. I expect that advanced filtering technique such as Gaussian and adaptive filtering will be applied using these data in the further research.

References

[1] J. G. Webster, *Design of Pulse Oximeter*. Taylor & Francis Group, 1997.

[2] N. Iftimia, William R. Brugge and D. X. Hammer, *Advances in Optical Imaging for Clinical Medicine*. John Wiley, 2010.

[3] Y. G. Lim, K. H. Hong, K. K. Kim, J. H. Shin, S. M. Lee, G. S. Chung, H. J. Baek, D. U. Jeong and K. S. Park, "Monitoring physiological signals using nonintrusive sensors installed in daily life equipment," *Biomedical Engineering Letters,* vol. 1, pp. 11-20, 2011.

[4] http://en.wikipedia.org/wiki/Optical_window_in_biological_tissue. (2011, 11.8).

[5] K. G. Humphreys, "An Investigation of Remote Non-Contact Photoplethysmography and Pulse Oximetery," Doctor of Philosophy, Department of Electronic Engineering, National University of Ireland, Maynooth, 2007.

[6] J. Bailey, M. Fecteau and Noah L. Pendleton, "Wireless Pulse Oximeter," Bachelor of Science, Worcester Polytechnics Institute, 2008.

[7] M. W. Wukitsch, M. T. Petterson, D. R. Tobler and J. A. Pologe, "Pulse Oximetery : Analysis of Theory, Technology, and Practice," *Journal of Clinical Monitoring and Computing,* vol. Vol 4., pp. 290 - 301, 1988.

[8] J. M. Lee, H. J. Beak and K. S. Park, "Oxygen Saturation Monitoring Without Direct Skin Contact : Preliminary Study," *u-Healthcare Conference,* 2011.

[9] J. Moyle, *Pulse Oximeter*. London: BMJ Publishing Group, 1994.

[10] K. J. Reynolds, E. Palayiwa, J. T. Moyle, M. K. Sykes and C. E. Hahn, "The effect of dyshemoglobins on pulse oximetry: Part Ⅰ, Theoretical approach and Part Ⅱ, Experimental results using an in vitro test system," *Journal of Clinical Monitoring,* vol. 9, pp. 81-90, 1993.

[11] P. L. Madsen and N. H. Secher, "Near-infrared Oximetry of the Brain," *Progress in neurobiology,* vol. 58, pp. 541-560, 1999.

[12] P. Rolfe, "In vivo Near-infrared Spectroscopy," *Annu Rev Biomed Eng,* vol. 2, pp. 715-754, 2000.

[13] E. Okada and D. T. Delpy, "Near-infrared Light Propagation in an Adult Head Model.," *Appl Opt,* vol. 42, pp. 2906-2914, 2003.

[14] C. E. Elwell, *A practical user guide to near-infrared spectroscopy*. London, UK, 1995.

[15] C. J. Soraghan, "Development of A Versatile Multichannel CWNIRS Intrument for Optical Brain-Computer Interface Applications," Doctor of Philosophy, Department of

Experimental Physics & Department of Computer Science, National University of Ireland, Maynooth, 2010.
[16] T. Muehlemann, D. Haensse and M. wolf, "Wireless Miniaturized in-vivo Near Infrared Imaging"," *Opt. Express,* vol. 16, 2008.
[17] M. Wolf, M. Ferrari and V. Quaresima, "Progress of Near-infrared Spectroscopy and Topography for Brain and Muscle Clinical Application," *J Biomed Opt,* vol. 12, pp. 62-104, 2007.
[18] G. Strangman, D. A. Boas and J. P. Sutton, "Non-invasive Neuroimaging using near-infrared Light," *Biol Psychiatry,* vol. 52, pp. 679-693, 2002.
[19] B. Chance, M. Cope, E. Gratton, N. Ramanujam and B. Tromberg, "Phase measurement of light absorption and scatter in human tissue," *Review of Scientific Instruments,* vol. 69, pp. 3457-3481, 1998.
[20] I. Y. Son, G. Markusand and W. D. Gray, "Human Performance Assessment using fNIRS," *Proceeding of SPIE,* 2006.
[21] D. Haensse, P. Szabo, D. Brown, J. Fauchere and P. Niederer, "New multichannel near infrared spectrophotometry system for functional studies of the brain in adults and neonates," *Opt. Express,* vol. 13, pp. 4525-4538, 2005.
[22] C. Soraghan, F. Matthews, C. Markham, B.A. Pearlmutter, R. O'Neill and T.E. Ward, "A 12-Channel, real-time near-infrared spectroscopy instrument for brain-computer interface applications," *30th Annual International IEEE EMBS Conference,* pp. 5648-5651, 2008.
[23] H. J. Beak, "Unconstrained PPG Measurement using Adaptive Light intensity Control," Degree of Master, Graduate Program in Bioengineering, Seoul National University, 2009.
[24] H. J. Baek, G. S. Chung, K. K. Kim, J. S. Kim and K. S. Park, "Photoplethysmogram Measurement Without Direct Skin-to-Sensor Contact Using an Adaptive Light Source Intensity Control," *IEEE TRANSACTIONS ON INFORMATION TECHNOLOGY IN BIOMEDICINE,* vol. 13, pp. 1085-1088, 2009.
[25] B. H. Choi, G. S. Chung, J. S. Lee, D. U. Jeong and K. S. Park "Slow-wave sleep estimation on a load-cell-installed bed: a non-constrained method," *Physiological Mesurement,* vol. 30, pp. 1163-1170, 2009.
[26] B. Lee, J. Han, H. J. Beak, J. H. Shin, K. S. Park and W. J. Yi, "Improved elimination of motion artifacts from a photoplethysmographic (PPG) signal using a Kalman smoother with simultaneous accelerometry", *Physiological Measurement,* Vol.31, No.12, pp.1585-1603, 2010

국문초록

무구속 Pulse Oxymetry와 휴대용 fNIRS 구현을 위한 광학적 생체신호 측정 시스템 개발

서울대학교 대학원
협동과정 바이오엔지니어링 전공
이 종 민

본 논문은 무구속적으로 생체 광학 신호를 모니터링 하기 위한 광학 측정 모듈 개발과 이 모듈의 무구속적 Pulse Oximetry와 휴대용 fNIRS 적용에 대하여 서술 하였다.

본 모듈은 발광부로는 Power LED, 수광부로는 PIN Diode를 기반으로 만들어 졌으며 Power LED는 Peak forward modulation 방식으로 구동하였다. Power LED는 760nm와 880nm 두 파장의 die 를 하나의 Package에 넣어 공간적 오차를 줄였다. 또한 빛에 세기와 측정되는 신호가 주변 환경에 적응하도록 Adaptive light intensity control 방법으로 빛이 세기를 조절하였다.

본 모듈을 적용하여 제작한 Non-intrusive Pulse Oximeter는 의자와 침대에 이식이 가능한 형태인 반사형으로 제작하였으며 SpO2는 각 파장의 흡광정도에 따른 Ratio of ratio를 이용하여 정성적으로 측정하였다. 실험은 각각 얇은 옷과 두꺼운 옷을 입은 상태에서 두 파장을 조사하여 반사되는 신호를 측정하는 방식으로 진행하였다.

실험 결과 두 파장의 신호를 분리하여 얻어 낼 수 있었으며, 각 신호의 high peak와 low peak 검출을 통한 SpO2의 계산, 심박동수 산출이 가능하였다. 또한 주변환경에 따라 빛의 세기가 자동으로 조절되어 측정되는 신호가 포화되거나 약해지는 것을 방지하는 것을 확인 할 수 있었다.

본 모듈을 이용하여 제작한 Portable fNIRS는 대뇌의 Frontal,

Motor cortex, Occipital 각 부분에 유연하게 적용할 수 있도록 발광부와 수광부를 분리하여 제작하였다.

시스템의 적용을 확인하기 위하여 Cz부분에 본 fNIRS 를 적용하고 시간을 달리하며 Finger Tapping 실험을 실시 하였으며, Finger tapping 구간과 Resting 구간 신호의 확연한 차이를 측정할 수 있었다.

주요어 : 휴대용, 무구속, 광학적 생체신호 측정, 산소포화도 측정, 기능적 근적외선 뇌활동도 측정 모듈
학 번 : 2010-23354